

A Deep Reinforcement Learning-based Approach for Adaptive Handover Protocols in Mobile Networks

Peter J. Gu , Johannes Voigt  and Peter M. Rost 

Communications Engineering Lab (CEL), Karlsruhe Institute of Technology (KIT), Hertzstr. 16, 76187 Karlsruhe, Germany
Email: peter.gu@student.kit.edu, {johannes.voigt, peter.rost}@kit.edu

Abstract—Due to an ever-increasing number of participants and new areas of application, the demands on mobile communications systems are continually increasing. In order to deliver higher data rates, enable mobility and guarantee QoS requirements of subscribers, these systems and the protocols used are becoming more complex. By using higher frequency spectrums, cells become smaller and more base stations have to be deployed. This leads to an increased number of handovers of user equipments between base stations in order to enable mobility, resulting in potentially more frequent radio link failures and rate reduction. The persistent switching between the same base stations, commonly referred to as “ping-pong”, leads to a consistent reduction of data rates. In this work, we propose a method for handover optimization by using proximal policy optimization in mobile communications to learn an adaptive handover protocol. The resulting agent is highly flexible regarding different travelling speeds of user equipments, while outperforming the standard 5G NR handover protocol by 3GPP in terms of average data rate and number of radio link failures. Furthermore, the design of the proposed environment demonstrates remarkable accuracy, ensuring a fair comparison with the standard 3GPP protocol.

Keywords—Communication Protocols, Handover, Mobility Management, Deep Reinforcement Learning

I. INTRODUCTION

The increasing number of users of wireless cellular networks and Internet of things (IoT) devices requires continuous adaptation and further development of mobile communication standards. Furthermore, the system is expected to perform reliably, flexibly, fast, and with low latency in order to meet the increasing demands [1]. Current mobile standards are approaching channel capacity, and an increase in data rate is only possible through an expansion of the spectrum towards higher frequencies. These frequencies experience significantly larger free-space path loss, leading to a substantial reduction in cell size and necessitating the deployment of numerous small base stations (BSs). This leads to the problem that a user equipment (UE), e.g., a smartphone, has to connect to more BSs while moving. If the UE moves between two BSs, the so-called handover (HO) process, which involves switching between BSs, can be redundantly executed. This effect is called *ping pong* (*PP*). Finding the ideal time steps to trigger HOs is an optimization problem due to the data rate being zero during HO processes.

In LTE and 5G NR, this challenge is tackled with a HO protocol, standardized by 3rd Generation Partnership Project (3GPP). This protocol uses fixed parameters, e.g. time-to-trigger (TTT), which limits the flexibility of it. However, there are several approaches trying to optimize parameters with machine learning (ML) models, e.g. [2]. In addition to

that, work has been done to avoid those fixed parameters using reinforcement learning (RL). Authors in [3] and [4] use a RL model with discretized states, for example connection power, which lead to inaccuracies for the learning agent. This issue can be solved using deep reinforcement learning (DRL), which is proposed in [5]. However, the training process is done on the UEs, which will reduce the battery life of the device drastically. Other approaches either use low UE speeds [6] or signal-to-interference-plus-noise ratio (SINR) instead of reference signal received power (RSRP) values as neural network (NN) input, although the decision process of the standardized protocol uses RSRP values. Guo et al. also use the proximal policy optimization (PPO) algorithm [7], but without a direct penalization of PPs and handover failures (HOFs) as we did in our work. Furthermore, there is no work that models the HO process properly to guarantee better comparability with the 3GPP protocol. Our work is capable of modelling the HO process in an accurate way, considering HO preparation and execution period, while the model is well comparable with the 3GPP protocol since only RSRP is used for training. In contrast to prior research that mainly concentrates on the HO problem itself, we further introduce the capability of RL models to operate at different UE speeds while outperforming the 3GPP protocol. This is all done with no additional training for different speeds. The source code is available at GitHub¹.

II. PRELIMINARIES

A. Handover Procedure in 5G NR

Similar to previous 3GPP releases, mobility in 5G NR is enabled by a mobility management function. The decision, as to which BS an UE is connected to or to which BS a handover is performed as soon as the UE leaves the serving cell, is made using an event-based protocol and is based on RSRP measurements. Depending on the serving cell RSRP and the RSRP of neighbouring cells, different events A1–A6 will be triggered [8, pp. 85 – 89]. Event A1 indicates that the RSRP of the serving BS is higher than a certain threshold, while event A2 is triggered if the RSRP is lower, respectively. The condition for a HO is satisfied when the RSRP of the serving BS falls below an acceptable threshold (event A2) and at the same time the RSRP of a neighbour BS exceeds the RSRP of the serving BS by a given hysteresis value (event A3). After a certain waiting time, TTT, the UE starts to transmit measurement reports to the serving BS, in which, e.g., RSRP measurements from various cells are reported. Based on these reports, a HO can be initiated by the serving BS.

¹The source code of this work is publicly available at: <https://github.com/kit-cel/HandoverOptimDRL>

The hysteresis, cell-dependent offsets and TTT are adjustable parameters and are used to avoid radio link failures (RLFs) and reduce PPs. If the serving BS becomes too weak and a HO is initiated too late, HOF can occur, resulting in RLFs. A RLF means that the UE is no longer synchronized with the network due to insufficient SINR. A HOF occurs when a HO process is aborted because the SINR of the serving or to-be-served BSs have been too low for an extended period.

B. Reinforcement Learning

In RL, an agent interacts with an environment and learns a strategy (policy) on which its actions are based on. The agent's actions are based on observations and states of the environment. For actions taken, the agent receives rewards from the environment on which the policy learning is based, where the agent's goal is to maximize both immediate and future rewards [9, pp. 1-5].

The following notation is used to describe the RL system: state $s \in \mathcal{S}$, $s' = s_{t+1}$, action $a \in \mathcal{A}$, transition (s, a, s') , the transition probability distribution $p(s'|s, a)$ and the reward $r(s, a) = r_t$ in time step t . In Fig. 1, the interaction between the agent and its environment is illustrated. The agent performs an action a_t in its environment. Subsequently, a new state s_{t+1} is reached and the agent receives a reward r_{t+1} for its selected action.

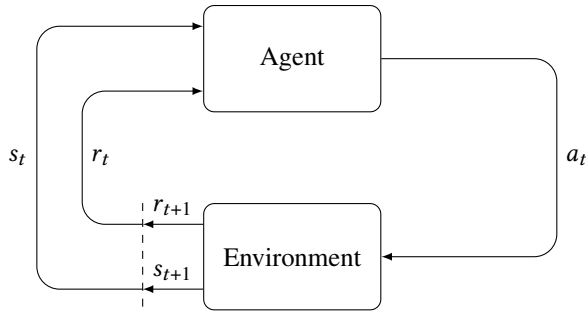


Fig. 1: Schematic of RL.

The agent follows a *policy* $\pi(a|s)$ and its goal is to maximize the expected future reward $\mathbb{E}_\pi \left[\sum_{k=0}^{\infty} \gamma^k r_{t+k} \right]$ with $\gamma \in [0, 1]$ as the discount factor. To evaluate the agent and thus the policy, the reward must be maximized. This reward is represented using the so-called *V-function* [9, p. 59]

$$V_t^\pi(s) = \mathbb{E}_\pi \left[\sum_{k=0}^{\infty} \gamma^k r_{t+k} | s_t = s \right] = \mathbb{E}_\pi \left[r_t + \sum_{k=1}^{\infty} \gamma^k r_{t+k} | s_t = s \right] \quad (1)$$

Besides several RL algorithms, there do exist algorithms which optimizations are based on the policy π . In PPO, two NNs, called actor net and critic net, are used. The actor net is responsible for action decision, while the critic net is involved in the calculation of the loss function.

With θ as the weights of the *actor net*, the calculation aims to select the policy that executes the optimal action a^* such that

$$\theta_{t+1} = \theta_t + \alpha \nabla_\theta \pi_\theta(a^* | s), \quad (2)$$

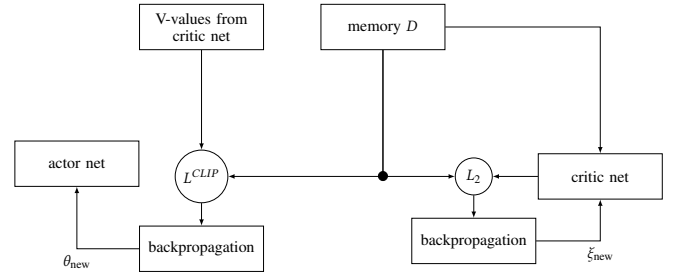


Fig. 2: Flow diagram visualizing the actor-critic update process.

where $\alpha \in \mathbb{R}$ is the learning rate. After normalization and gradient weighting, this will lead to the commonly used estimator² [10], [11]

$$\hat{g} = \hat{\mathbb{E}}_t \left[\nabla_\theta \log \pi_\theta(a_t | s_t) \hat{A}_t \right], \quad (3)$$

with the advantage function $\hat{A}_t = \hat{A}(s_t | a_t) = Q^\pi(s_t, a_t) - V^\pi(s_t)$ [11]. For calculating the V-values, the *critic net* with its weights ξ is used. As stated in [11], the probability ratio $\psi_t(\theta) = \frac{\pi_\theta(a_t | s_t)}{\pi_{\theta_{old}}(a_t | s_t)}$ is used for the estimator stated in Eq. 3. Next, authors in [11] introduce the surrogate loss function used for PPO

$$L^{\text{CLIP}} = \hat{\mathbb{E}}_t \left[\min \left(\psi_t(\theta) \hat{A}_t, \text{clip}(\psi_t(\theta), 1 - \epsilon, 1 + \epsilon) \hat{A}_t \right) \right]. \quad (4)$$

This loss function can prevent excessively large update steps. By using $\epsilon \in (0, 1)$ in this equation, the new policy π_θ is constrained to not deviate too far from the old policy $\pi_{\theta_{old}}$.

Now the actor-critic update process is roughly described. In the first step, the agent explores trajectories and store the resulting actions, rewards, and states into memory D , which can be obtained in Fig. 2. In the second step, V-values are delivered by the critic net while the net itself is updated via some gradient descent algorithm L_2 , e.g. mean squared error (MSE). In the third step, the actor net can be updated with those V-values, following the objective L^{CLIP} [12].

III. HANDOVER OPTIMIZATION PROBLEM

To achieve the highest data rate, one possibility is to immediately switch to the strongest BS. However, as explained earlier, the data rate is zero during the HO execution, which must be taken into consideration. Thus, a low number of PPs and HOFs is desirable. Furthermore, the optimal time for triggering a HO has to be identified to prevent RLFs.

IV. SYSTEM MODEL

For the generation of RSRP and SINR traces of an UE moving through an environment, the *Vienna 5G System Level Simulator* [13] is used. An area of downtown Karlsruhe³ is used for simulations in this work. Overall, five 5G NR macro BSs are distributed over the map, as it is shown in Fig. 3. Furthermore, the *QuaDRiGa* [14] channel model is used to simulate the link between an UE and the base stations. Information about the environment, such as floor plans of buildings

²This derivation step is not trivial. A good explanation can be found in [10].

³Coordinates: 49°00'17.6"N 8°22'38.3"E – 49°00'40.3"N 8°23'44.2"E

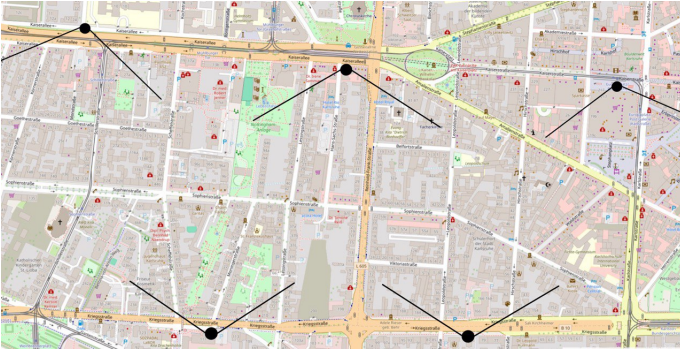


Fig. 3: Simulation area of Karlsruhe with 5 BSs. The black circles represent the BS, while the lines indicate the direction of the beam.

and streets, is obtained via OpenStreetMap. UEs are modelled such that they move only on streets at different speeds and thereby representing different user groups, e.g., pedestrians, cyclists and inner-city car traffic. The simulated RSRP and SINR values are validated by comparing the distributions of the generated data with the distributions of measurement data in an urban area based on publicly available measurements of the 5G campus network in Kaiserslautern [15].

A. RL Environment Design

1) *Simulation of Ping-Pongs*: For simulation purposes, 3GPP suggests a minimum connection duration of an UE with a BS, referred to as the minimum time of stay (MTS) [16]. When a second HO occurs within a time interval shorter than MTS to the former BS, it is referred to as PP.

2) *Simulation of Handover Failures*: To simulate HOF, [16] refers to the following method: to detect a HOF, a monitoring process runs concurrently beside the HO procedure. If the SINR is worse than a configured threshold Q_{out} , indicating an unsynchronized communication link, timer T310 is initiated. Two situations may arise:

- If the HO preparation is completed, and a handover is executed while the timer is running, a HOF is triggered as shown in Fig. 4.
- If timer T310 expires before a HO can be executed, a HOF is triggered.

Timer T310 can be stopped and reset if the SINR exceeds a configured threshold Q_{in} during this operation. When a HOF is triggered, the UE undergoes a RLF recovery process lasting multiple time steps. During this period, the UE is not connected to any BS. It establishes a new connection to a BS, where this phase is called RLF recovery.

B. Simulation Overall

To ensure a fair comparison with the HO protocol of 3GPP, its rules and constraints, as explained earlier, have been met and consolidated. The resulting algorithm is illustrated in Alg. 1.

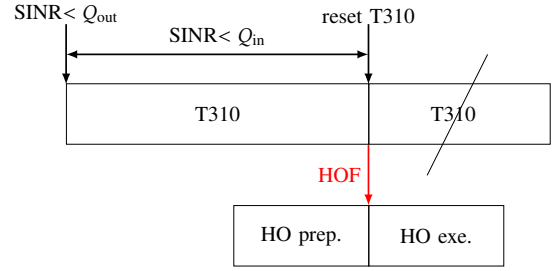


Fig. 4: HOF triggered after HO preparation.

C. Pseudo RSRQ

As mentioned before, only RSRP values will be utilized in the HO decision process to ensure high compatibility with the existing 3GPP protocol. To further address issues related to interference power, a *pseudo reference signal received quality (RSRQ)* is used. The RSRQ is defined in [17] as:

$$RSRQ = N \cdot \frac{RSRP}{RSSI}, \quad (5)$$

where N is the number of resource blocks used and received signal strength indicator (RSSI) is the average-received power in a single orthogonal frequency division multiplexing (OFDM) symbol. The measurement also includes the power of neighbouring BSs. Thus, this equation can be simplified as the ratio of the RSRP of the serving BS to the sum of RSRP values from all interfering BSs. If there exist $B = |\mathcal{B}|$ BSs, with indices $b = 0, 1, \dots, B-1$, Eq. 5 can be simplified to:

$$RSRQ_{pseudo,b} = \frac{RSRP_b}{\sum_{i=0, i \neq b}^{B-1} RSRP_i}.$$

For simplicity, $RSRQ_{pseudo}$ will be abbreviated as RSRQ in the following sections.

D. State and Action Design

The state $s \in \mathcal{S} = [\vec{s}_{one-hot}, \vec{SINR}_{norm}, \vec{s}_{add}]$ consists of three parts. The first component is a one-hot encoding vector $\vec{s}_{one-hot}$, indicating to which BS the UE is currently connected. All bits in the binary vector are set to '0', except for one bit which is set to '1' [18], e.g. $\vec{s}_{one-hot,b=1} = [0, 1, 0]$ with $B = 3$.

The second part is composed of normalized and clipped RSRQ values of all BSs in one time step. RSRQ is clipped between -10 dB and 10 dB to strengthen the focus on usable link quality and to eliminate ambiguities in finding the strongest BS. These values are described as:

$$RSRQ_{norm} = \begin{cases} 1, & \text{if } RSRQ \geq 10 \text{ dB} \\ 0, & \text{if } RSRQ \leq -10 \text{ dB} \\ \frac{RSRQ+10}{20}, & \text{else.} \end{cases}$$

The clipping and the normalization are done to improve the learning performance of the NN [19].

The third part \vec{s}_{add} is introduced to inform the NN whether a PP is possible. This is accomplished with

$$\vec{s}_{add} = \begin{cases} 1, & \text{if } t - t_{HO} < MTS \\ 0, & \text{else,} \end{cases}$$

Algorithm 1

```
1: if RLF recovery not in progress then
2:   if T310 in progress then
3:     if T310 expired then
4:       Trigger HOF
5:     else
6:       if HO execution pending then
7:         Trigger HOF
8:       else
9:         if SINR >  $Q_{in}$  then
10:          Reset T310
11:        end if
12:      end if
13:    end if
14:  else
15:    if HO over then
16:      if SINR of new BS <  $Q_{out}$  then
17:        Trigger HOF
18:      end if
19:    else
20:      if SINR <  $Q_{out}$  then
21:        Start T310
22:      else
23:        Reset T310
24:      end if
25:    end if
26:  end if
27: end if
```

with the current time step t and the time step of the last HO t_{HO} . This allows the agent to better identify whether a PP or a HOF is responsible for a negative reward. The state s is the input of the NN.

The actions $a \in \mathcal{A} = \{0, 1, \dots, B-1\}$ serve as indicators of the preferred BS to which the agent aims to establish a connection. This is obtained from the output of the NN.

E. Reward Design

If the UE runs into a RLF recovery, the agent should be penalized by a constant $C \in \mathbb{R}^+$, as well as if PPs are detected or the SINR of the BS is less than Q_{out} . Avoiding situations where $SINR < Q_{out}$ is important to get rid of too late HO, in which the SINR becomes too low, triggering timer T310 and resulting in an RLF. Moreover, the time needed for RLF-recovery is significantly longer than the HO execution time. So its penalty is twice as high as in the case of a HO. Upon successful HO, the reward r defined in Eq. 6 is increased by C to acknowledge a successful HO.

$$r = \begin{cases} RSRQ_{norm} + C, & \text{UE connected to the strongest BS} \\ RSRQ_{norm}, & \text{UE is connected to a strong, but not} \\ & \text{the strongest BS} \\ -C, & \text{UE is connected to a BS with} \\ & \text{SINR} < Q_{out} \\ -C, & \text{PP detected} \\ -2 \cdot C, & \text{UE is not connected, RLF recovery} \end{cases} \quad (6)$$

F. Training Process

In each epoch, a random dataset, which is uniformly distributed, will be chosen for training. Each data set consists of both SINR and RSRP values of all BSs. While SINR is used only for monitoring purposes (see Ch. IV-A2), it is not utilized for RL training. To enhance diversity in the data, BS-RSRP/SINR mappings are randomly selected in every epoch during training. Since actions cannot be executed during HO execution or RLF recovery, those time steps will be skipped. During training, the agent gets terminated if either HOFs or PPs occur. The following chapter provides a more detailed explanation of the learning algorithm.

G. Learning Algorithm

In the first step, weights of actor and critic net have to be initialized. After selecting a data set and shuffling it, the agent will explore various trajectories, generating samples as it selects actions and store them in a memory D [12][20]. If this is done, the objectives explained in Ch. II-B are executed. The exploration will be terminated in case of HOFs or PPs. As a consequence, the agent must begin exploring the dataset from time step 0. The learning algorithm of the model can be found in Alg. 2.

Algorithm 2

```
1:  $\theta \leftarrow$  Initialize weights of actor net
2:  $\xi \leftarrow$  Initialize weights of critic net
3: for episode  $i$  do
4:   Choose one dataset and shuffle the RSRP/SINR
   mapping
5:   The agent explores trajectories of the environment,
   generates  $m$  samples  $(s, a, s', r)$ , and stores them in the
   memory  $D$ 
6:   for 1 to  $m/n$  do
7:     Choose a data set batch consisting of  $n$  samples
8:     Calculate V values of the critic net
9:     for each sample with its corresponding V value do
10:      Calculate the V value using the current critic
      net to get  $\hat{A}$ .
11:       $\theta \leftarrow \theta_{new}$  with  $L^{CLIP}$ 
12:       $\xi \leftarrow \xi_{new}$ 
13:      if HOF or PP occurs then
14:        Termination – reset environment to time
        step 0
15:      end if
16:    end for
17:  end for
18:  Clear the memory  $D$ 
19: end for
```

V. PERFORMANCE EVALUATION

A. Experimental Setup

After generating SINR and RSRP values using the Vienna 5G Simulator [13] for 15 different trajectories in the area described in Ch. IV, the PPO agent will undergo training, utilizing Python and Stable Baselines3 (SB3) library⁴ [21].

⁴Source code has been adjusted to disable mini-batch shuffling to stabilize training

10 routes are for training and 5 for testing. The UEs moves at a speed of 50 km/h for exactly 3 minutes each. With a sample interval of 120 ms, this will result in 1500 time steps. 120 ms has been chosen to align with the report interval standardized by 3GPP [8]. The duration of certain events, such as the preparation/execution of HOs, is shorter than the sample interval. In order to correctly represent these events, the samples generated using the Vienna 5G Simulator are interpolated such that the temporal resolution is 10 ms. This interpolation is achieved using the Fourier method. To mitigate Fourier side effects, a moving average filter with a length of 2 s is applied to the data.

For both, actor and critic network, the same network architecture of the hidden layers is used. While the first and third hidden layers consist of 64 neurons, the second hidden layer comprises 128 neurons. The ReLU activation function is employed in both the input layer and all hidden layers, whereas no activation function is utilized in the output layer.

The training process consists of three training iterations. First, the agent will randomly choose the entropy coefficient $\text{ent}_{\text{coef}} \in \{0.1, 0.01, 0.001\}$ and the constant $C \in [0.6, 0.95]$. With those two parameters, the first iteration is executed on all datasets. To accelerate the learning process, all data sets are reduced to 1 min for the initial and subsequent learning phase. Furthermore, the environment will only be reset if a HOF occurs. The learning rate is set to $5 \cdot 10^{-5}$ for the first 500 epochs. In the second iteration, the learning rate is set to 10^{-6} for further 300 epochs. In the last iteration the training will be executed on the whole dataset of 3 min with the same learning rate and number of epochs as in iteration 2. Additionally, the environment will now also be reset if a PP occurs. In all three iterations, the learning rate decreases linearly until it reaches zero after the last epoch.

The evaluation of the learned agent is conducted on five traces of an UE moving through the streets of the simulated area for each of the considered velocities: 3 km/h, 30 km/h, and 50 km/h. Finally, the agent is trained with a UE moving at 50 km/h, but is also evaluated at speeds of 30 km/h and 3 km/h without additional training required.

In the next section, the performance of the PPO agent is evaluated and compared to the existing 5G NR HO protocol implemented using Python 3.10 and following Alg. 1. Three metrics are tracked: the mean data rate and the number of HOFs and PPs. The mean data rate is compared to the mean of the maximum data rate at each time step i . This involves taking the logarithm of the respective maximum SINR at each time step and subsequently computing the overall average [22, p. 13]. After obtaining the ratio of the SINR values between the connected BS and the BS with the maximum SINR, the mean data rate is calculated as follows:

$$\Gamma = \frac{\sum_{i=0}^{\Lambda-1} \log_2(1 + \text{SINR}_i)}{\sum_{i=0}^{\Lambda-1} \max_{b \in \mathcal{B}} \log_2(1 + \text{SINR}_{i,b})},$$

with the total number of time steps Λ .

B. Simulation Results

We compare the trained PPO agent with the standard 3GPP protocol. The parameters used by the 3GPP protocol

are illustrated in Tab. I. For an accurate model of the 3GPP handover procedure, the HO preparation and execution time, timer T310, Q_{in} , Q_{out} , RLF recovery and MTS are also used in the environment of the PPO setup. Further parameters, tuned with Weights & Biases (W&B) [23] can be obtained from Tab. II.

TABLE I: Parameters used for 3GPP protocol [2][16].

Parameter	Value
A2 threshold	-80 dBm
A2 hysteresis	1 dB
A3 hysteresis	1 dB
HO preparation time	50 ms
HO execution time	40 ms
T310	1000 ms
TTT	160 ms
Q_{out}	-8 dB
Q_{in}	-6 dB
RLF recovery	200 ms
MTS	1000 ms
Offset	2 dB

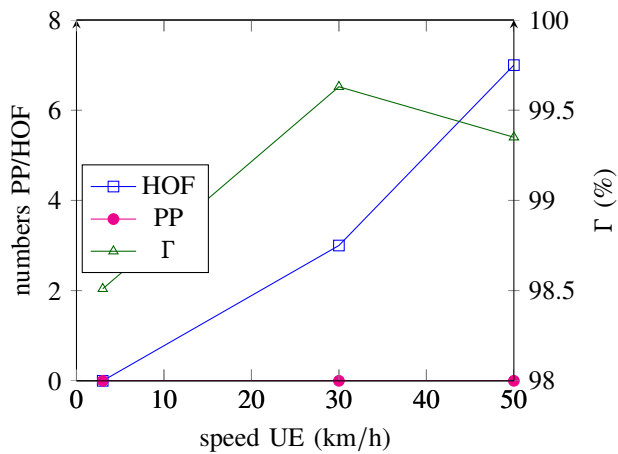
TABLE II: PPO agent related parameters.

Parameter	Value
ent_{coef}	0.1
C	0.9405
batch size iteration 1 and 2	150
batch size iteration 3	550

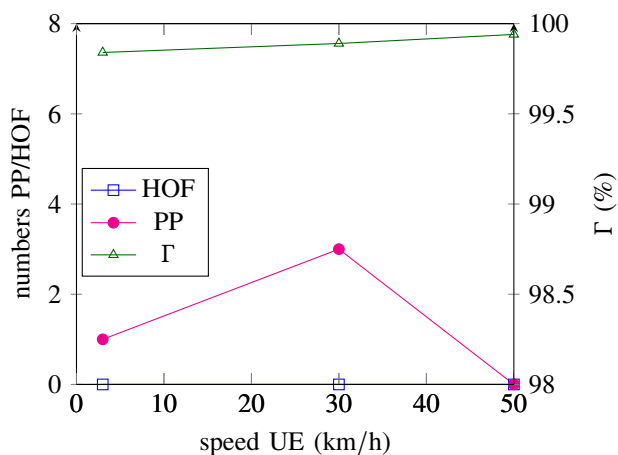
Figure 5 shows the simulation results of one evaluation dataset used for both the 3GPP protocol and the PPO agent. The three metrics HOF, PP and Γ are plotted for three different UE speeds. On this dataset, the 3GPP protocol does not have any problems with PPs but the number of HOFs increases with higher UE speeds. Compared to the 3GPP protocol, the PPO agent is able to trigger the HOs such that no HOFs occurs. However, some PPs occur in this case. It must be noted that the definition of a PP is not unambiguous, and therefore the number of PPs occurred depends on the MTS defined in [16]. Moreover, the mean data rate achieved by the PPO agent consistently exceeds that of the 3GPP protocol. This trend is reflected in the metric Γ , which is consistently higher for the PPO agent.

VI. CONCLUSION

In this paper, we investigated a new method for learning adaptive HO protocols by using PPO. Our results show that a RL-based HO protocol can outperform the standard protocol by 3GPP in terms of mean data rate and number of RLFs. The adaptivity of the RL agent to varying environment conditions is remarkable, e.g., different user velocities, without changing any parameters or additional training for different conditions.



(a) 3GPP protocol



(b) PPO agent

Fig. 5: Simulation results for the 3GPP protocol and the PPO agent for one evaluation data set.

The HO decisions of the agent are based on RSRP measurements without using further information about the simulated area or the positions of the UE and the BSs, to ensure a fair comparison to the 3GPP protocol. For the comparison of our model to the standard protocol, we implemented an abstraction of the 3GPP standard, including the HO preparation and execution time as well as timers for RLF detection.

REFERENCES

- [1] J. G. Andrews, S. Buzzi, W. Choi, S. V. Hanly, A. Lozano, A. C. K. Soong, and J. C. Zhang, "What Will 5G Be?" *IEEE Journal on Selected Areas in Communications*, vol. 32, no. 6, pp. 1065–1082, Jun. 2014.
- [2] D. Castro-Hernandez and R. Paranjape, "Optimization of Handover Parameters for LTE/LTE-A in-Building Systems," *IEEE Transactions on Vehicular Technology*, vol. 67, no. 6, pp. 5260–5273, Jun. 2018.
- [3] V. Yajnanarayana, H. Rydén, and L. Hévízi, "5G Handover using Reinforcement Learning," in *2020 IEEE 3rd 5G World Forum (5GWF)*, Sep. 2020, pp. 349–354.
- [4] Q. Liu, C. F. Kwong, S. Wei, L. Li, and S. Zhang, "Intelligent Handover Triggering Mechanism in 5G Ultra-Dense Networks Via Clustering-Based Reinforcement Learning," *Mobile Networks and Applications*, vol. 26, no. 1, pp. 27–39, Feb. 2021.

- [5] Y. Cao, S.-Y. Lien, Y.-C. Liang, and K.-C. Chen, "Federated Deep Reinforcement Learning for User Access Control in Open Radio Access Networks," in *ICC 2021 - IEEE International Conference on Communications*, Jun. 2021, pp. 1–6.
- [6] M. Mollel, S. Kajjage, and K. Michael, "Deep Reinforcement Learning based Handover Management for Millimeter Wave Communication," 2021.
- [7] D. Guo, L. Tang, X. Zhang, and Y.-C. Liang, "Joint Optimization of Handover Control and Power Allocation Based on Multi-Agent Deep Reinforcement Learning," *IEEE Transactions on Vehicular Technology*, vol. 69, no. 11, pp. 13 124–13 138, Nov. 2020.
- [8] "Specification #: 38.331." [Online]. Available: <https://portal.3gpp.org/desktopmodules/Specifications/SpecificationDetails.aspx?specificationId=3197>
- [9] R. S. Sutton and A. G. Barto, *Reinforcement Learning: An Introduction*, 2nd ed. The MIT Press, 2018.
- [10] A. L. Ecoffet. (2018) An Intuitive Explanation of Policy Gradient. [Online]. Available: <https://towardsdatascience.com/an-intuitive-explanation-of-policy-gradient-part-1-reinforce-aa4392cbfd3c>
- [11] J. Schulman, F. Wolski, P. Dhariwal, A. Radford, and O. Klimov, "Proximal Policy Optimization Algorithms," Aug. 2017, arXiv:1707.06347 [cs]. [Online]. Available: <http://arxiv.org/abs/1707.06347>
- [12] OpenAI, "Openai spinning up - proximal policy optimization," 2020. [Online]. Available: <https://spinningup.openai.com/en/latest/algorithms/ppo.html>
- [13] M. K. Müller, F. Ademaj, T. Dittrich, A. Fastenbauer, B. Ramos Elbal, A. Nabavi, L. Nagel, S. Schwarz, and M. Rupp, "Flexible multi-node simulation of cellular mobile communications: the Vienna 5G System Level Simulator," *EURASIP Journal on Wireless Communications and Networking*, vol. 2018, no. 1, p. 227, Sep. 2018.
- [14] "QuaDRiGa." [Online]. Available: <https://quadriga-channel-model.de/>
- [15] S. B. Mallikarjun, C. Schellenberger, C. Hobelsberger, and H. D. Schotten, "Performance Analysis of a Private 5G SA Campus Network," in *Mobile Communication - Technologies and Applications; 26th ITG-Symposium*, May 2022, pp. 1–5.
- [16] "Specification #: 36.839." [Online]. Available: <https://portal.3gpp.org/desktopmodules/Specifications/SpecificationDetails.aspx?specificationId=2540>
- [17] F. Afroz, R. Subramanian, R. Heidary, K. Sandrasegaran, and S. Ahmed, "SINR, RSRP, RSSI and RSRQ Measurements in Long Term Evolution Networks," *International Journal of Wireless & Mobile Networks*, vol. 7, no. 4, pp. 113–123, Aug. 2015.
- [18] F. Harrag and S. Gueliani, "Event extraction based on deep learning in food hazard arabic texts," *CoRR*, vol. abs/2008.05014, 2020. [Online]. Available: <https://arxiv.org/abs/2008.05014>
- [19] J. Coholich, "A Bag of Tricks for Deep Reinforcement Learning," May 2022. [Online]. Available: https://jmccoholich.github.io/post/rl_bag_of_tricks/
- [20] X. B. P., P. Abbeel, S. Levine, and M. van de Panne, "Deepmimic: Example-guided deep reinforcement learning of physics-based character skills," 2018.
- [21] A. Raffin, A. Hill, A. Gleave, A. Kanervisto, M. Ernestus, and N. Dornmann, "Stable-baselines3: reliable reinforcement learning implementations," *The Journal of Machine Learning Research*, vol. 22, no. 1, pp. 268:12 348–268:12 355, Jan. 2021.
- [22] J. G. Proakis and M. Salehi, *Digital communications*, 5th ed., ser. McGraw-Hill higher education. Boston [u.a.]: McGraw-Hill, 2009.
- [23] L. Biewald, "Experiment tracking with weights and biases," 2020, software available from wandb.com. [Online]. Available: <https://www.wandb.com/>